

DYNAMIC APERTURE OF JLEIC ELECTRON COLLIDER RING WITH ERRORS AND CORRECTION*

Y. Nosochkov[†], Y. Cai, SLAC National Accelerator Laboratory, Menlo Park, CA, USA
 F. Lin, V. Morozov, Y. Zhang, Jefferson Lab, Newport News, VA, USA

Abstract

Design of the Jefferson Lab Electron-Ion Collider (JLEIC) includes low-beta Interaction Region (IR) and spin rotator optics for high luminosity and polarization. Magnet errors, especially in the high-beta final focus quadrupoles, result in optics perturbations which need to be corrected in order to attain sufficient dynamic aperture (DA). We present design of orbit correction system for the electron ring and evaluate its performance. The DA is then studied including misalignment, magnet strength errors, non-linear field errors, and corrections.

INTRODUCTION

The Jefferson Lab Electron-Ion Collider (JLEIC) [1] is designed to attain high luminosity and beam polarization. The design is based on a figure-8 layout as shown in Fig. 1. This feature provides an optimal preservation of the ion and electron polarization [2]. The 2.3-km electron and ion rings are stacked vertically in the tunnel; they cross each other horizontally at the Interaction Point (IP) at 50 mrad angle, where $\beta_x^* = 10$ cm, $\beta_y^* = 2$ cm. Second IP can be added in the opposite straight in the future. The rings are compatible with the energy range of 3 – 12 GeV for electrons and 30 – 200 GeV for protons.

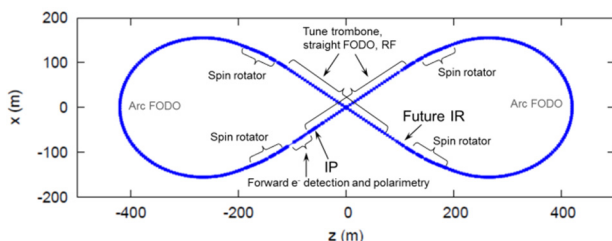


Figure 1: Layout of the JLEIC electron collider ring.

Magnet errors cause various optics perturbations which need to be corrected in order to achieve sufficient dynamic aperture (DA), and the specified luminosity and polarization. In this study, we design orbit correction system for the electron ring and evaluate its performance. Then, detailed tracking simulations are performed to study dynamic aperture with misalignment, magnet strength errors, non-linear field errors, and the corresponding corrections. Error tolerances are discussed.

LATTICE

The electron collider ring consists of two arcs and two long straight sections. The latter include Interaction Re-

gion (IR), two vertical doglegs combined with spin rotators, RF-cavities, tune trombones, and a polarimeter chicane. Each arc is made of short 11.4-m FODO cells with high 108° phase advance. This choice provides low 4.6 nm-rad emittance at 5 GeV. The above cell phase advance also provides cancellation of second-order effects from periodic sextupoles in every 10 cells due to +I transformation [3]. For this reason, chromaticity correction scheme consists of two-family periodic sextupoles in 40 cells of each arc. The electron ring optics functions are shown in Fig. 2, where tune is $Q_x = 57.22$, $Q_y = 50.16$.

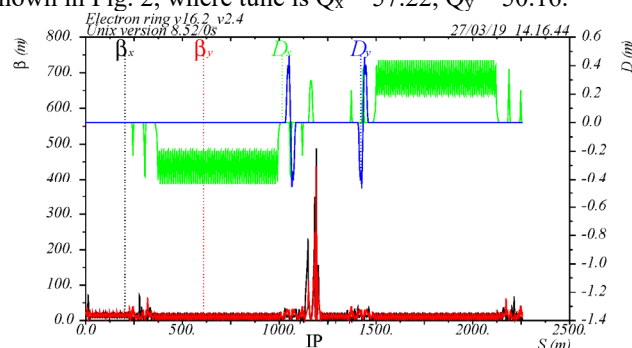


Figure 2: Optics functions of the electron collider ring.

ERRORS AND ORBIT CORRECTION

Magnet errors such as X and Y offsets, roll angles, magnet strength errors, and higher order multipole field errors cause a variety of optics perturbations including distortion of orbit, dispersion and beta functions, transverse coupling, chromaticity, tune shift, and non-linear effects. These effects may lead to poor dynamic aperture and short beam lifetime; hence, they must be corrected. The most sensitivity is to errors in the strong final focus quadrupoles (FFQ), where beta functions are very large. Comparison of orbit response from the FFQ and the nearby quadrupoles due to 0.2 mm offsets is shown in Fig. 3.

To compensate the orbit distortion due to magnet misalignment and dipole field errors, we design the orbit correction system consisting of horizontal (X) and vertical (Y) dipole correctors and dual-plane monitors (BPM). For minimum corrector strength and maximum response, the X and Y correctors are typically placed near focusing and defocusing quadrupoles, respectively, where the corresponding beta functions are high. Each corrector is 30 cm long and the BPM is 5 cm long. The corrector distribution is optimized to avoid redundant locations where phase advance between the correctors is too small. Sufficient number of correctors and BPMs is included in the IR, shown in Fig. 4, to minimize the strong impact of the FFQ misalignment in the IP area. There are total of 213 X-correctors, 191 vertical correctors and 474 BPMs. This

* Work supported by the U.S. Department of Energy, Office of Science, and Office of Nuclear Physics under Contracts DE-AC05-06OR223177, DE-AC02-06CH11357, and DE-AC02-76SF00515.

[†] yuri@slac.stanford.edu

system is designed to perform global orbit correction. To navigate beams into collision at the IP, a dedicated local correction is planned to be used consisting of pairs of X and Y correctors on each side of IP. This system is not part of this study.

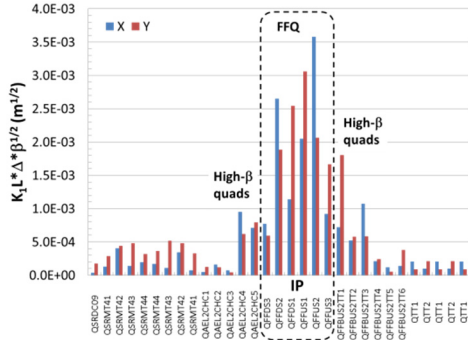


Figure 3: Orbit response from the electron ring quadrupoles near IP, misaligned by $\Delta = 0.2$ mm.

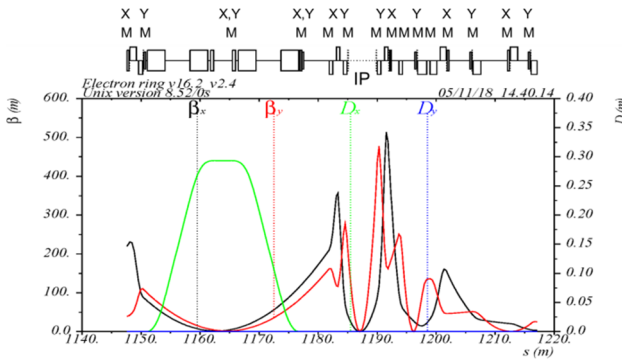


Figure 4: Optics functions and locations of orbit correctors (X,Y) and BPMs in the electron ring IR.

Typical errors used in this study are listed in Tables 1 and 2; they are based on the errors from PEP-II CDR study and the PEP-II measured field [4]. The alignment errors are even more conservative than the PEP-II errors. The random multipoles shown in Table 2 are the rms values; in simulations, these components are generated within $\pm 3\sigma$ range. The use of the PEP-II measured multipole field is justified since there is a plan to reuse the PEP-II magnets in the electron ring. The multipole errors in the study include only normal components since there are no skew components in the available PEP-II data.

Table 1: RMS Magnet Offset, Roll Angle and Strength Error in this Study, where the gaussian distribution is cut at 3σ

	X,Y (mm)	Roll (mrad)	$\Delta B/B$ (%)
Dipole	0.2	0.5	0.1
Quadrupole	0.2	0.5	0.1
Sextupole	0.2	0.5	0.2
FFQ	0.2	0.5	0.05

Orbit correction is simulated using LEGO code [5]. The orbit after correction with the misalignment in Table 1 is shown in Fig. 5 for 10 seeds of random errors. The rms and maximum corrector strengths at 12 GeV are about

25 Gm and 145 Gm, respectively, which should be achievable. Smaller X,Y misalignment proportionally reduces the corrected orbit and the corrector strengths. However, the DA improvement is minimal. Hence, we choose the conservative misalignment in Table 1 as preliminary tolerances; the latter also apply to the FFQ misalignment.

Table 2: Measured Normal Field Multipoles b_n (10^{-4} units) of PEP-II HER Magnets at Reference Radius R

	n	Systematic	n	Random
Dipole R = 30 mm	3	0.1	3	0.32
	4	0	4	0.32
	5	0	5	0.64
	6	0	6	0.82
Quadrupole R = 44.9 mm	3	10.3	3	5.6
	4	5.6	4	4.5
	5	4.8	5	1.9
	6	23.7	6	1.7
	10	-31.0	10	1.8
	14	-26.3	14	0.7
Sextupole R = 56.52 mm	9	-145	5	22
	15	-130	7	10.5

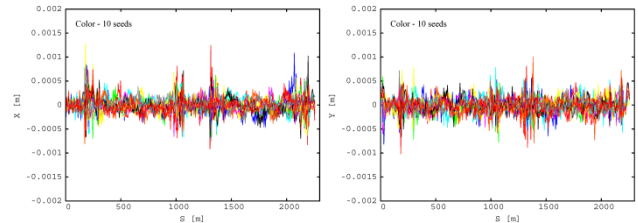


Figure 5: X,Y orbit correction with Table 1 misalignment for 10 seeds of random errors (IP is at S = 0).

DYNAMIC APERTURE

Dynamic aperture is obtained using particle tracking in LEGO. The simulations are performed for 10 seeds of random errors including corrections, where the errors are generated within $\pm 3\sigma$ range. The DA is calculated at the IP at 13 angles in X-Y space (0 to 180°) in 2000-turn tracking at 5 GeV. It is expressed in units of rms beam size (σ), where horizontal emittance is 4.6 nm-rad, and the vertical emittance is based on emittance ratio of 5:1. Synchrotron oscillations and effects of non-linear fringe field in quadrupoles and dipoles are included. The RF voltage is 2.579 MV. Linear chromaticity is corrected to +1 using the two-family arc sextupoles.

To compensate various optics distortions caused by the misalignment and field errors, the simulations include the following corrections to compensate: global orbit (using dipole correctors and BPMs), betatron tune (2-family arc quadrupoles), linear chromaticity, vertical dispersion (Y-correctors), beta functions (various quadrupoles), global coupling (sextupole vertical offsets). SVD method is used for the orbit, dispersion, coupling and beta function corrections to find the most efficient set of correctors.

To avoid unstable optics due to application of large errors, the errors in the simulations are increased gradually,

Content from this work may be used under the terms of the CC BY 3.0 licence (© 2019). Any distribution of this work must maintain attribution to the author(s), title of the work, publisher, and DOI

in small steps, while doing the corrections at each step, until the specified error values are reached.

For reference, the DA without errors is shown in Fig. 6, where DA at various momentum offsets $\Delta p/p$ is also given. The on-momentum DA is $15\sigma_x \times 45\sigma_y$ which is sufficient; and the momentum range is $\sim 8\sigma_p$ ($\sigma_p = 4.6 \cdot 10^{-4}$).

DA for 10 seeds of alignment errors from Table 1, including the corrections, is shown in Fig. 7. The minimum DA in 10 seeds is $14.5\sigma_x \times 44\sigma_y$ – nearly the same as without errors. This indicates that as long as the misalignment effects are corrected, the impact on the DA is small. Residual rms optics distortions after corrections are: orbit < 0.2 mm, $\Delta\beta < 3$ m, $\Delta\beta^*/\beta^* < 3\%$, $\Delta D_x < 3$ cm, $\Delta D_y < 5$ mm, where $D_{x,y}$ is dispersion.

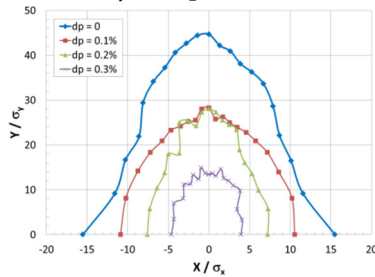


Figure 6: Electron ring DA without errors vs $\Delta p/p$.

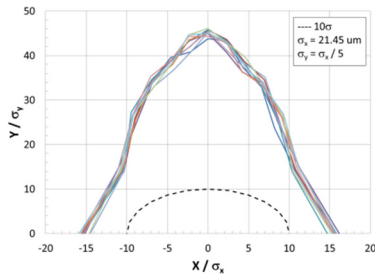


Figure 7: DA with alignment errors from Table 1 and corrections for 10 seeds of random errors.

Figure 8 shows the DA for both misalignment and PEP-II measured multipole errors, with corrections, for 10 seeds of random errors. The minimum DA is $10.1\sigma_x \times 41.5\sigma_y$, where the horizontal DA is reduced by $\sim 4\sigma_x$ relative to the DA in Fig. 7 due to the multipole field errors. Note that these errors are applied to all magnets including the more sensitive FFQ magnets.

Finally, the DA is calculated with all the errors in Tables 1 and 2, including the misalignment, multipole field errors, and the magnet strength errors. The same rms errors are applied to all magnets, except the magnet strength errors in six FFQ magnets are reduced a factor of two relative to other magnets. This is due to difficulty in error correction for some random seeds because of the strong FFQ effects. The reduced 0.05% rms strength error in the FFQ is still quite conservative. The resulting DA is presented in Fig. 9. The minimum DA is $9.4\sigma_x \times 40.6\sigma_y$, where the X-aperture is reduced by $0.7\sigma_x$ relative to the DA in Fig. 8.

The DA with all the errors in Tables 1 and 2 is slightly below 10σ . This may be sufficient, but further improve-

ment is desired. The used errors are quite conservative; they can be considered as preliminary tolerances for most magnets. The DA could be improved by assigning more stringent tolerances to the FFQ magnets as typically done in colliders. The FFQ will be the new superconducting magnets, hence one could aim at a better FFQ field quality than in Table 2. An example of scaling of the PEP-II multipole field in the FFQ is shown in Fig. 10. In this case, a factor of 2 reduction of the PEP-II multipole field in the FFQ increases the DA by $\sim 1\sigma_x$ to $10.4\sigma_x$. The DA improvement is also expected with implementation of planned multipole field correctors in the FFQ.

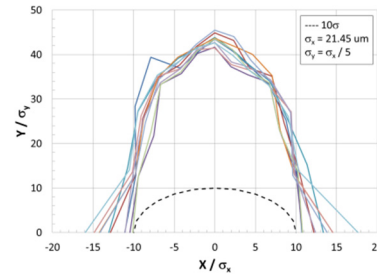


Figure 8: DA with misalignment and PEP-II multipole field errors and corrections, for 10 seeds of random errors.

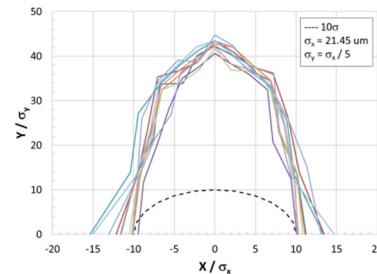


Figure 9: DA with misalignment, magnet strength errors, and multipole field errors, for 10 seeds of random errors.

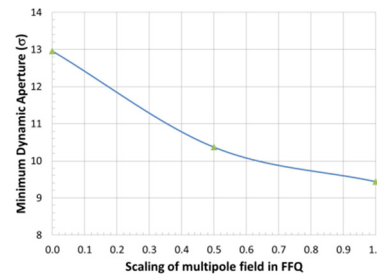


Figure 10: DA with all errors vs multipole field errors in the FFQ, scaled from the PEP-II errors.

CONCLUSION

Orbit correction system designed for the electron collider ring shows acceptable performance resulting in minimal DA degradation with conservative alignment errors. The DA with misalignment, magnet strength errors and PEP-II measured multipole field errors is almost 10σ which may be sufficient. The DA could be increased by a better field quality in the new superconducting FFQ magnets, other optics improvements, and implementation of multipole field correctors in the FFQ.

REFERENCES

- [1] S. Abeyratne *et al.*, “MEIC design summary”, 2015, http://casa.jlab.org/MEICSumDoc1-2015/MEIC_Summary_Document_1-2015.pdf
- [2] Ya.S. Derbenev, University of Michigan report UM HE 96-05, 1996.
- [3] K.L. Brown, “A second-order magnetic optical achromat,” *IEEE Trans.Nucl.Sci.*, vol. 26, pp. 3490-3492, 1979.
- [4] PEP-II Conceptual Design Report, SLAC-418, June 1993.
- [5] Y. Cai, M. Donald, J. Irwin, and Y. Yan, “LEGO: a modular accelerator design code”, SLAC-PUB-7642, 1997.